# Modal Identities for Multibody Elastic Spacecraft

Hari B. Hablani*
*Rockwell International, Seal Beach, California 97040*

**This paper answers the question, Which set of modes furnishes a higher fidelity math model of dynamics of a multibody, deformable spacecraft—hinges-free or hinges-locked vehicle modes? Three sets of general, discretized, linear equations of motion of a spacecraft with an arbitrary number of deformable appendages, each articulated directly to the core body, are obtained using the above two families of modes and appendage modes. By a comparison of these equations, 11 sets of matrix and scalar modal identities are constructed that involve modal momenta coefficients and frequencies associated with the three classes of modes. The sums of infinite series that appear in the identities are obtained in terms of mass and first and second moments of inertia of the appendages, core body, and vehicle by using some basic identities concerning appendage modes. Applying the above identities to a four-body spacecraft, the hinges-locked vehicle modes are found to yield a higher fidelity model than hinges-free modes because the hinges-free modes have nondiminishing modal coefficients, whereas the hinges-locked modes have modal angular momentum coefficients diminishing rapidly with frequency. These characteristics are proved in the paper.**

## I. Introduction

DYNAMIC models of elastic spacecraft in the 1970s and early 1980s were usually based on appendage or vehicle modes, with the spacecraft modeled as a central rigid body and appendages cantilevered to it. Likins et al.[1] and Hughes and Skelton[2] established several criteria for selecting appendage or vehicle modes in order to construct high fidelity and yet low-order dynamic models of the spacecraft. Some of these criteria are based on modal identities[3,4] that were illustrated in detail in Refs. 4 and 5. In contrast to these relatively simple vehicles, the spacecraft on drawing boards today are considerably more complicated, significantly more deformable, and have several articulated flexible appendages—NASA's Space Station for example. The dynamic interaction between the spacecraft bus and the hinged bodies or cantilevered appendages can be modeled either in terms of classical appendage modes or in terms of relatively less known hinges-free or hinges-locked vehicle modes.[6] By definition, hinges-free modes are obtained by leaving all hinges free—unlocked and unforced; the associated natural vehicle modes therefore may contain motion of the articulated bodies relative to the inboard bodies. Conversely, in the case of hinges-locked modes, the relative motion of the articulated bodies is, by definition, zero, and some force or torque is applied at the hinge to keep the motion so. In Ref. 6, these vehicle modes are formulated for NASA's Space Station, and their zero linear and angular momentum properties, the orthogonality conditions, and the associated modal momenta coefficients are theorized. The principal objective of this paper, in line with the objectives of Refs. 1–4, is to determine whether hinges-free or hinges-locked vehicle modes furnish a higher fidelity dynamic model, if the same number of modes are retained in a simulation. To this end, a multibody spacecraft is considered that consists of a rigid core body and $N$ flexible appendages, each articulated directly to the core body. Three sets of discrete motion equations for this spacecraft are obtained from a continuum set using appendage modes, hinges-free vehicle modes, and hinges-locked vehicle modes. To compare the last two families of modes, modal identities are devised, following Hughes,[3] that express the sum of the contributions of all infinite number of modes in terms of first and second moments of inertia of the articulated bodies, the core body, and the vehicle. The analysis is amply illustrated, and definitive conclusions are summarized at the end of the paper. Although, for concreteness, this paper considers a multibody spacecraft with level 1 articulated bodies, it will be clear that the conclusions drawn apply to a wider range of multibody spacecraft.

## II. Formulation of Continuum Equations of Motion

Figure 1 portrays an $N+1$-body spacecraft that consists of a three-axis stabilized core rigid body $B_0$, and deformable bodies $E_1,...,E_N$, each articulated directly to the core body. The motion equations will be developed with respect to the reference point 0 in Fig. 1, which is neither the mass center $\oplus_0$ of the body $B_0$, nor the mass center $\oplus$ of the entire vehicle $V$. This generality in the formulation is warranted because the NASTRAN modal data corresponding to such

**Hari B. Hablani received his M.E. and Ph.D. in Aeronautical Engineering in 1978 from the Indian Institute of Science, Bangalore, India. He was then a postdoctoral fellow in the Department of Aeronautics and Astronautics at Purdue University, West Lafayette, Indiana for two years. Subsequently, he was a NASA National Research Council Associate for two years at Johnson Space Center, Houston, Texas. Since 1982 he has been with the Guidance and Control Group, Rockwell International, Satellite and Space Electronics Division, Seal Beach, California. His field of specialization is the dynamics and control of multibody flexible spacecraft.**

Received Feb. 17, 1989; revision received Aug. 14, 1989. 

*Engineering Specialist, Guidance and Control Group. AIAA Senior Member.

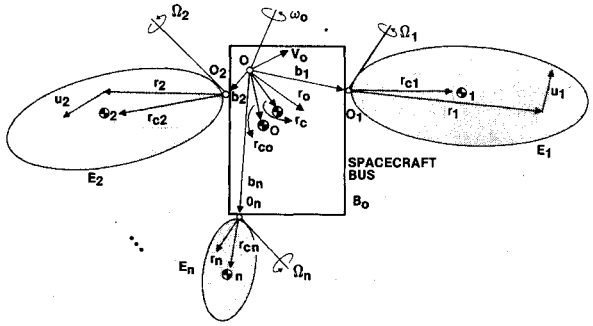


**Fig. 1 $N+1$-body spacecraft with $N$ articulated, deformable appendages.**

multibody spacecraft are often with respect to an arbitrary reference node 0, and the mass centers are generally nodeless, empty points. The mass of each body is denoted $m_p$ $(p=0,1,...,N)$, the mass of all $N$ articulated bodies together $m_e$, and the mass of the entire spacecraft $m_j$; clearly, $m=m_0+m_e$. The first moment of mass of $B_0$ relative to 0 is $c_0=m_0 r_{c0}$, and those for the hinged bodies $(j=1,\ldots,N)$, measured from the respective hinges $0_j$, are denoted $c_j=m_j r_{cj}$. Similar to $c_p$ $(p=0,1,...,N)$, the vector $r_0$ emanates from 0 and $r_j$ from $0_j$. Note that the subscript $p$ covers all bodies, whereas $j$ covers only the articulated bodies. The vectors $b_j$ $(j=1,...,N)$ originating from 0 locate the hinges $0_j$ of the hinged bodies $E_j$. The first moment of inertia of the entire spacecraft, then, is

$$c=c_0+\sum_j (m_j b_j + C_{0j}c_j) \triangleq c_0+c_e; \quad \sum_j = \sum_{j=1}^{N} \tag{1}$$

where the matrix $C_{0j}$ transforms the $E_j$-fixed vector $c_j$ to a $B_0$-fixed vector, and the vectors $b_j$ are expressed in the $B_0$-fixed frame. Next, $J_0$ denotes the inertia matrix of the body $B_0$ about the reference point 0, while $J_j$ is the inertia matrix of the hinged body $E_j$ in its own frame about the hinge $0_j$. The inertia matrix of $E_j$ expressed at the reference point 0 in the $B_0$-fixed frame is denoted $J_j^0$ and

$$J_j^0 = C_{0j}J_jC_{j0} - [m_j b_j^{\times} b_j^{\times} + b_j^{\times}(C_{0j}c_j)^{\times} + (C_{0j}c_j)^{\times} b_j^{\times}] \tag{2}$$

where $(\cdot)^{\times}$ means the $3\times 3$ skew-symmetric matrix associated with the vector $(\cdot)$. The inertia matrix $J$ of the entire vehicle at the point 0 will then be

$$J = J_0 + \sum_j J_j^0 \triangleq J_0 + J_e^0 \tag{3}$$

Anticipating our later needs, the cross inertia matrix $J_{0j}$ between the bodies $B_0$ and $E_j$ expressed in the $E_j$-fixed frame equals

$$J_{0j} \triangleq J_j - (C_{j0}b_j)^{\times}c_j^{\times} \tag{4}$$

As for the motion of the spacecraft, its center is assumed to perform some orbital motion not coupled with its attitude motion under consideration. To develop motion equations, the local orbital frame is taken to be an inertial frame. The kinetic quantities of interest are as follows: $V_0(t)$, the perturbational velocity of the reference point 0 over the uniform orbital motion at time $t$; $\omega_0(t)$, the inertial angular velocity of $B_0$; $\Omega_j(t)$, the angular velocity of each articulated body $E_j$ relative to $B_0$ at the hinge $0_j$; and $u_j(r_j,t)$, the deformation of $E_j$ at the location $r_j \varepsilon E_j$. These quantities are taken to be linear, first order, and infinitesimal, so their products can be ignored in the analysis. The external forces and torques acting on the spacecraft are the force $f_0(t)$ and torque $g_0(t)$ acting on $B_0$ at 0, and the force $f_j(t)$ and the torque $g_j(t)$ on each $E_j$ at the hinge $0_j$. The latter pair $(f_j,g_j)$ includes a distributed force $f_j(r_j,t)$ acting in the domain of the body $E_j$. Regarding the control forces and torques, those acting on $B_0$ are included in the quantities $f_0,g_0$, whereas, if a control force or torque is produced in the interior domain of $E_j$ without acting against the core body $B_0$, then that is included in the pair $(f_j,g_j)$; however, if a control torque is produced by an electric motor that rests on $B_0$ at the interface $0_j$ and exerts the torque on $E_j$, then this is considered separately and denoted $g_{0j}(t)$ $(j=1,...,N)$, for it produces a reaction torque $-g_{0j}(t)$ that acts on $B_0$. The total force $f(t)$ and torque $g(t)$ that act on the vehicle are

$$f=f_0+\sum_j C_{0j}f_j, \quad g=g_0+\sum_j (C_{0j}g_j + b_j^{\times}C_{0j}f_j) \tag{5}$$

where, of course, $g(t)$ does not include the control torque $g_{0j}(t)$ at the interface $0_j$.

The elastic spacecraft under consideration is relatively simple; it is straightforward to develop its linear, continuum motion equations following Hughes.[3,7,8] The equations governing the discrete variables $V_0,\omega_0,\Omega_j$ $(j=1,...,N)$ are

$$m\dot{V}_0 - c^{\times}\dot{\omega}_0 - \sum_j C_{0j}c_j^{\times}\dot{\Omega}_j + \sum_j \int_j C_{0j}\ddot{u}_j \, dm = f$$

$$c^{\times}\dot{V}_0 + J\dot{\omega}_0 + \sum_j C_{0j}J_{0j}\dot{\Omega}_j + \sum_j \int_j (b_j^{\times}C_{0j} + C_{0j}r_j^{\times})\ddot{u}_j \, dm = g$$

$$c_j^{\times}C_{j0}\dot{V}_0 + (C_{0j}J_{0j})^T\dot{\omega}_0 + J_j\dot{\Omega}_j + \int_j r_j^{\times}\ddot{u}_j \, dm = g_{0j} + g_j \quad (j=1,...,N) \tag{6}$$

where an overdot indicates differentiation with respect to time, $\int_j \triangleq \int_{E_j}$, and $(\cdot)^T$ means transpose of the quantity $(\cdot)$. To write the motion equation governing the deformation $u_j(r_j,t)$ of the flexible body $E_j$, denote the related linear stiffness operator by $L_j$; the body $E_j$ is allowed to be anisotropic and/or nonhomogeneous, and its mass density is denoted $\sigma_j(r_j)$. The continuum motion equation governing the deformation $u_j$ is then:

$$L_j u_j + \sigma_j[C_{j0}\dot{V}_0 - (C_{j0}b_j + r_j)^{\times}C_{j0}\dot{\omega}_0 - r_j^{\times}\dot{\Omega}_j + \ddot{u}_j] = f_j(r_j,t)$$

$$(j=1,...,N) \tag{7}$$

The continuum motion equations [Eqs. (6) and (7)] are discretized in the next section.

## III. Discretization of Continuum Equations of Motion

Three families of modes will be employed in this section for discretization: 1) appendage modes, 2) hinges-free vehicle modes, and 3) hinges-locked vehicle modes. The use of appendage modes is standard; they are employed here in order to evaluate the infinite sums that appear in the hinges-free and hinges-locked modal identities in Section IV in terms of mass and first and second moments of inertia of the appendages, core body and the vehicle.

### Discretization via Appendage Modes

Following Hughes,[3] define the modal momenta coefficients $P_{j\sigma}$ and $H_{j\sigma}$ concerning the appendage (cantilever) modes $U_{j\sigma}^a(r_j)$ of the articulated body $E_j$:

$$P_{j\sigma} \triangleq \int_j U_{j\sigma}^a(r_j) \, dm$$

$$H_{j\sigma} \triangleq \int_j r_j^{\times}U_{j\sigma}^a(r_j) \, dm \quad (j=1,...,N)\ (\sigma=1,...,\infty) \tag{8}$$

where $dm$ is elemental mass. The coefficient $P_{j\sigma}$ is associated with linear momentum and $H_{j\sigma}$ with angular momentum of the mode $\sigma$ at the hinge point $0_j$. The modal angular momen-

tum coefficient relative to the reference point 0 (Fig. 1) is defined as

$$H^0_{j\sigma} \triangleq b_j^{\times} C_{0j} P_{j\sigma} + C_{0j} H_{j\sigma} \tag{9}$$

Then the continuum equations [Eqs. (6) and (7)] discretize to

$$m\dot{V}_0 - c^{\times}\dot{\omega}_0 - \sum_j C_{0j} c_j^{\times} \dot{\Omega}_j + \sum_j C_{0j} \sum_\sigma P_{j\sigma} \ddot{Q}_{j\sigma} = f$$

$$c^{\times}\dot{V}_0 + J\dot{\omega}_0 + \sum_j C_{0j} J_{0j} \dot{\Omega}_j + \sum_j \sum_\sigma H^0_{j\sigma} \ddot{Q}_{j\sigma} = g$$

$$c_j^{\times} C_{j0} \dot{V}_0 + J^T_{0j} C_{j0} \dot{\omega}_0 + J_j \dot{\Omega}_j + \sum_\sigma H_{j\sigma} \ddot{Q}_{j\sigma} = g_j + g_{0j}$$

$$P^T_{j\sigma} C_{j0} \dot{V}_0 + H^{0T}_{j\sigma} \dot{\omega}_0 + H^T_{j\sigma} \dot{\Omega}_j + \ddot{Q}_{j\sigma} + \Omega^{c2}_{j\sigma} Q_{j\sigma} = \gamma^a_{j\sigma} \tag{10}$$

$$(j = 1,...,N;\ \sigma = 1,...,\infty)$$

where $Q_{j\sigma}(t)$ is the modal coordinate and $\Omega^c_{j\sigma}$ the frequency associated with the $\sigma$th appendage mode $U^a_{j\sigma}(r_j)$ of the body $E_j$; $\gamma^a_{j\sigma}(t)$ is the modal input to $\sigma$th mode:

$$\gamma^a_{j\sigma}(t) = \int_j U^{aT}_{j\sigma}(r_j) f_j(r_j,t)\, dA \tag{11}$$

with $dA$ denoting elemental area. Equations (10) are a generalization of Eqs. (35) of Hughes,[3] for the former includes articulation motion of the appendages and the latter do not. In Sec. IV, Eqs. (10) will be used in developing modal identities. To facilitate matrix manipulations, they are abbreviated by using the definitions

$$C^{0T}_A \triangleq -[C_{01}c_1^{\times},...,C_{0N}c_n^{\times}],\quad J^T_{0A} \triangleq [C_{01}J_{01},...,C_{0N}J_{0N}]$$

$$P^T_j \triangleq [...P_{j\sigma}...],\quad P^{0T}_A \triangleq [C_{01}P^T_1,...,C_{0N}P^T_N]$$

$$H^{0T}_j \triangleq [...H^0_{j\sigma}...],\quad H^{0T}_A \triangleq [H^{0T}_1,...,H^{0T}_N]$$

$$H^T_j \triangleq [...H_{j\sigma}...],\quad H_A \triangleq \text{diag}[H_1...H_N],\quad J_A \triangleq \text{diag}[J_1...J_N]$$

$$Q^T_j \triangleq [...Q_{j\sigma}...],\quad Q^T_A \triangleq [Q^T_1...Q^T_N]$$

$$g^T_A \triangleq [g^T_1...g^T_N],\quad g^T_{0A} \triangleq [g^T_{01}...g^T_{0N}],\quad \Omega^T_A \triangleq [\Omega^T_1...\Omega^T_N]$$

$$\Omega^c_j \triangleq \text{diag}[...\Omega^c_{j\sigma}...],\quad \Omega_c \triangleq \text{diag}[\Omega^c_1...\Omega^c_N]$$

$$\gamma^{aT}_j \triangleq [...\gamma^a_{j\sigma}...],\quad \gamma^{aT}_A \triangleq [\gamma^{aT}_1...\gamma^{aT}_N] \tag{12}$$

Furthermore, we define

$$M_{VV} \triangleq \begin{bmatrix} m\mathbf{1} & -c^{\times} \\ c^{\times} & J \end{bmatrix} \quad M_{VA} \triangleq [C^0_A \quad J_{0A}],\quad \ddot{q}^T_V \triangleq [\dot{V}^T_0 \quad \dot{\omega}^T_0]$$
$$\mathscr{P}^0_A \triangleq [P^0_A \quad H^0_A],\quad u^T_V \triangleq [f^T \quad g^T] \tag{13}$$

where $\mathbf{1}$ is a $3 \times 3$ identity matrix. Equations (10) then reduce to the following three matrix equations: one governing six overall degrees of freedom of the spacecraft, $q_V(t)$; the second governing $n_a \times 1$ vector $\Omega_A$ of $n_a$ relative angular velocities of $N$ articulated bodies ($n_a$ equals the total number of articulation degrees of freedom); and the third governing the $\infty \times 1$ vector $Q_A$ of modal coordinates of appendage modes of all articulated bodies.

$$M_{VV}\ddot{q}_V + M^T_{VA}\dot{\Omega}_A + \mathscr{P}^{0T}_A \ddot{Q}_A = u_V(t) \tag{14a}$$

$$M_{VA}\ddot{q}_V + J_A\dot{\Omega}_A + H^T_A\ddot{Q}_A = g_A(t) + g_{0A}(t) \tag{14b}$$

$$\mathscr{P}^0_A\ddot{q}_V + H_A\dot{\Omega}_A + \ddot{Q}_A + \Omega^2_c Q_A = \gamma^a_A(t) \tag{14c}$$

Modal identities associated with the modal momenta matrices $\mathscr{P}^0_A$ and $H_A$ are derived in Section IV.

**Discretization via Hinges-Free Vehicle Modes**

In this technique, the continuum equations [Eqs. (6) and (7)] are discretized all at once. For this purpose, the following modal expansion is postulated for the variables in Eqs. (6) and (7)[6]

$$V_0(t) = \dot{R}_0(t) + \sum \chi_{0v}\dot{\eta}_v(t),\quad \omega_0(t) = \dot{\Theta}_0(t) + \sum \Phi_{0v}\dot{\eta}_v(t),$$

$$\sum = \sum_{v=1}^{\infty}$$

$$\Omega_j(t) = \dot{\Theta}_j(t) + \sum \Phi_{jv}\dot{\eta}_v(t),\quad u_j(r_j,t) = \sum U_{jv}(r_j)\eta_v(t),$$

$$(j = 1,2,...,N) \tag{15}$$

where $R_0, \Theta_0$, and $\Theta_j$ are the temporal coordinates for the rigid modes of the spacecraft—$n_a + 6$ rigid modes in all. Furthermore, $R_0$ is the translation of the reference point 0, and $\Theta_0$ is the rotation of the spacecraft, both in rigid modes; similarly, $\Theta_j$ is the rotation of the hinged body $E_j$ relative to $B_0$ at the hinge $0_j$ ($j = 1,...,N$) in a rigid mode. The quantities $\chi_{0v}$, $\Phi_{0v}$, and $\Phi_{jv}$ ($j = 1,...,N$; $v = 1,...,\infty$) are $v$th modal coefficients contributing, respectively, to the overall discrete motions $V_0, \omega_0$, and $\Omega_j$, and $\eta_v(t)$ is the associated modal coordinate. The eigenfunction $U_{jv}(r_j)$ is that part of the hinges-free vehicle mode, denoted $W_v(r)$, which defines the deformation of body $E_j$ in the $v$th mode. Although $U_{jv}(r_j)$ satisfies the condition of zero displacement and zero slope at the hinge $0_j$, that is, $U_{jv}(0_j) = 0$ and $(1/2)\nabla^{\times} U_{jv}(0_j) = 0$, it is not the same as the $\sigma$th appendage mode $U^a_{j\sigma}(r_j)$ used before, because in the case of $U_{jv}(r_j)$ no torque acts, by definition, at the hinge $0_j$ to enforce the zero deformation and slope condition, whereas in the case of $U^a_{j\sigma}(r_j)$ the immobile support of the appendage enforces that condition. Because of the mobile support of the hinge $0_j$, the total motion $W_{jv}(r_j)$ of $E_j$ in an inertial frame is

$$W_{jv}(r_j) = \chi_{0v} - (b_j + C_{0j}r_j)^{\times}\Phi_{0v} - C_{0j}r_j^{\times}\Phi_{jv} + C_{0j}U_{jv}(r_j) \quad (j = 1,...,N;\ v = 1,...,\infty) \tag{16}$$

where the first two terms in the right side result from the translation and rotation of the core body in the $v$th mode, and the third term $r_j^{\times}\Phi_{jv}$ results from the relative rotation of $E_j$ at the free hinge $0_j$. The motion of the core body in $v$th mode is given simply by

$$W_{0v}(r_0) = \chi_{0v} - r_0^{\times}\Phi_{0v} \tag{17}$$

Thus the hinges-free vehicle mode $W_v(r)$ spans the entire spacecraft such that

$$W_v(r) = \begin{cases} W_{0v}(r_0), & \text{if } r = r_0 \\ W_{jv}(r_j), & \text{if } r = b_j + C_{0j}r_j \end{cases} \quad (j = 1,...,N;\ v = 1,...,\infty) \tag{18}$$

The $6 + n_a$ rigid modes of a spacecraft with articulated bodies are $\mathbf{1}$, $-r^{\times}$, and $-r_j^{\times}$ ($j = 1,...,N$) (retain only those columns in $-r_j^{\times}$ that correspond to the free axes at the hinge $0_j$). Not surprisingly, the elastic modes $W_v(r)$ ($v = 1,...,\infty$) are orthogonal to these rigid modes, that is,

$$\int_V W_v(r)\, dm = 0 \tag{19a}$$

$$\int_V r^{\times} W_v(r)\, dm = 0 \tag{19b}$$

$$\int_j r_j^{\times} C_{j0} W_{jv}(r_j)\, dm = 0 \tag{19c}$$

where $\int_V$ means the entire vehicle is the domain of integration. Equations (19) can be verified by substituting the expansion [Eq. (15)] in the continuum equations [Eqs. (6)] with zero right sides. Indeed, Eqs. (19a) and (19b) state that the linear and angular momentum residing in a $v$th hinges-free vehicle mode are zero, whereas Eq. (19c) states that the angular momentum of the total motion $\boldsymbol{W}_{jv}(\boldsymbol{r}_j)$ of the $j$th articulated body in $v$th mode at the hinge $0_j$ is zero. These properties can be stated alternately by defining modal momenta coefficients $(\boldsymbol{p}_{jv},\boldsymbol{h}_{jv})$ for each articulated body and $(\boldsymbol{p}_v,\boldsymbol{h}_v^0)$ for all articulated bodies collectively:

$$\boldsymbol{p}_{jv} \triangleq \int_j \boldsymbol{U}_{jv}(\boldsymbol{r}_j)\,\mathrm{d}m \qquad \boldsymbol{h}_{jv} \triangleq \int_j \boldsymbol{r}_j^{\times}\boldsymbol{U}_{jv}(\boldsymbol{r}_j)\,\mathrm{d}m$$

$$\boldsymbol{p}_v \triangleq \sum_j \boldsymbol{C}_{0j}\boldsymbol{p}_{jv} \qquad \boldsymbol{h}_v^0 = \sum_j (\boldsymbol{b}_j^{\times}\boldsymbol{C}_{0j}\boldsymbol{p}_{jv} + \boldsymbol{C}_{0j}\boldsymbol{h}_{jv}) \tag{20}$$

where $\boldsymbol{h}_v^0$ is defined relative to the reference point 0. These may be compared with the definitions [Eqs. (8) and (9)]. The zero momentum properties [Eq. (19)] then transform to:

$$m\boldsymbol{\chi}_{0v} - \boldsymbol{c}^{\times}\boldsymbol{\Phi}_{0v} - \sum_j \boldsymbol{C}_{0j}\boldsymbol{c}_j^{\times}\boldsymbol{\Phi}_{jv} + \boldsymbol{p}_v = \boldsymbol{0}$$

$$\boldsymbol{c}^{\times}\boldsymbol{\chi}_{0v} + \boldsymbol{J}\boldsymbol{\Phi}_{0v} + \sum_j \boldsymbol{C}_{0j}\boldsymbol{J}_{0j}\boldsymbol{\Phi}_{jv} + \boldsymbol{h}_v^0 = \boldsymbol{0}$$

$$\boldsymbol{c}_j^{\times}\boldsymbol{C}_{j0}\boldsymbol{\chi}_{0v} + \boldsymbol{J}_{0j}^T\boldsymbol{C}_{j0}\boldsymbol{\Phi}_{0v} + \boldsymbol{J}_j\boldsymbol{\Phi}_{jv} + \boldsymbol{h}_{jv} = \boldsymbol{0}$$

$$(j = 1,\ldots,N;\ v = 1,\ldots,\infty) \tag{21}$$

The eigenvalue problem and the orthogonality conditions that govern hinges-free vehicle modes are recorded in the companion paper.[9]

Using the modal expansion [Eq. (15)], the zero momentum modal properties [Eqs. (19) and (21)], and the orthogonality properties, the continuum equations are discretized to these decoupled equations that separately govern the rigid and elastic modes of the spacecraft:

$$m\ddot{\boldsymbol{R}}_0 - \boldsymbol{c}^{\times}\ddot{\boldsymbol{\Theta}}_0 - \sum_j \boldsymbol{C}_{0j}\boldsymbol{c}_j^{\times}\ddot{\boldsymbol{\Theta}}_j = \boldsymbol{f} \tag{22a}$$

$$\boldsymbol{c}^{\times}\ddot{\boldsymbol{R}}_0 + \boldsymbol{J}\ddot{\boldsymbol{\Theta}}_0 + \sum_j \boldsymbol{C}_{0j}\boldsymbol{J}_{0j}\ddot{\boldsymbol{\Theta}}_j = \boldsymbol{g} \tag{22b}$$

$$\boldsymbol{c}_j^{\times}\boldsymbol{C}_{j0}\ddot{\boldsymbol{R}}_0 + \boldsymbol{J}_{0j}^T\boldsymbol{C}_{j0}\ddot{\boldsymbol{\Theta}}_0 + \boldsymbol{J}_j\ddot{\boldsymbol{\Theta}}_j = \boldsymbol{g}_{0j} + \boldsymbol{g}_j \quad (j = 1,\ldots,N) \tag{22c}$$

$$\ddot{\eta}_v + \omega_v^2\eta_v = \boldsymbol{\chi}_{0v}^T\boldsymbol{f} + \boldsymbol{\Phi}_{0v}^T\boldsymbol{g} + \sum_j \boldsymbol{\Phi}_{jv}^T(\boldsymbol{g}_{0j} + \boldsymbol{g}_j) + \gamma_v(t)$$

$$(v = 1,2,\ldots,\infty) \tag{22d}$$

where $\omega_v$ is the frequency of $v$th mode and $\gamma_v(t)$ is the scalar input to it considering all articulated bodies collectively:

$$\gamma_v(t) \triangleq \sum_j \int_j \boldsymbol{U}_{jv}^T(\boldsymbol{r}_j)\boldsymbol{f}_j(\boldsymbol{r}_j,t)\,\mathrm{d}A \tag{23}$$

These equations are abbreviated by recalling appropriate definitions from Eqs. (12) and (13) and by the following additional definitions

$$\boldsymbol{q}_{VR} \triangleq \begin{bmatrix}\boldsymbol{R}_0\\ \boldsymbol{\Theta}_0\end{bmatrix},\quad \boldsymbol{\Theta}_A \triangleq \begin{bmatrix}\boldsymbol{\Theta}_1\\ \vdots\\ \boldsymbol{\Theta}_N\end{bmatrix}$$

$$\boldsymbol{\chi}_0 \triangleq \begin{bmatrix}\vdots\\ \boldsymbol{\chi}_{0v}^T\\ \vdots\end{bmatrix},\quad \boldsymbol{\Phi}_0 \triangleq \begin{bmatrix}\vdots\\ \boldsymbol{\Phi}_{0v}^T\\ \vdots\end{bmatrix},$$

$$\boldsymbol{\Phi}_A \triangleq \begin{bmatrix}\vdots & & \vdots\\ \boldsymbol{\Phi}_{1v}^T & \cdots & \boldsymbol{\Phi}_{Nv}^T\\ \vdots & & \vdots\end{bmatrix}$$

$$\boldsymbol{\eta}_e^T \triangleq [\ldots\eta_v\ldots],\quad \boldsymbol{\omega} \triangleq \mathrm{diag}[\ldots\omega_v\ldots],\quad \boldsymbol{\gamma}^T \triangleq [\ldots\gamma_v\ldots] \tag{24}$$

Here $\boldsymbol{q}_{VR}$ is a vector of rigid motion of the vehicle, whereas $\boldsymbol{q}_V$ in Eq. (13) is a vector of overall motion; the vectors $\dot{\boldsymbol{\Theta}}_A$ in Eq. (24) and $\boldsymbol{\Omega}_A$ in Eq. (12) differ likewise. Equations (22) now condense to:

$$\boldsymbol{M}_{VV}\ddot{\boldsymbol{q}}_{VR} + \boldsymbol{M}_{VA}^T\ddot{\boldsymbol{\Theta}}_A = \boldsymbol{u}_V$$

$$\boldsymbol{M}_{VA}\ddot{\boldsymbol{q}}_{VR} + \boldsymbol{J}_A\ddot{\boldsymbol{\Theta}}_A = \boldsymbol{g}_A + \boldsymbol{g}_{0A}$$

$$\ddot{\boldsymbol{\eta}}_e + \boldsymbol{\omega}^2\boldsymbol{\eta}_e = \boldsymbol{\chi}_0\boldsymbol{f} + \boldsymbol{\Phi}_0\boldsymbol{g} + \boldsymbol{\Phi}_A(\boldsymbol{g}_{0A} + \boldsymbol{g}_A) + \boldsymbol{\gamma} \tag{25}$$

Compare these with Eqs. (14).

#### Discretization by Hinges-Locked Vehicle Modes

These modes are defined by forcing the articulation motion $\boldsymbol{\Omega}_j$ $(j = 1,\ldots,N)$ to be zero, so they are obtained by a modal analysis of the first two equations in Eqs. (6) and Eq. (7) from which the $\dot{\boldsymbol{\Omega}}_j$ $(j = 1,\ldots,N)$ terms are ignored. The torque actually required to keep the hinges locked can be evaluated from the third equation in Eq. (6) but that is not attempted here. The equations for the modal analysis are therefore:

$$m\dot{\boldsymbol{V}}_0 - \boldsymbol{c}^{\times}\dot{\boldsymbol{\omega}}_0 + \sum_j \int_j \boldsymbol{C}_{0j}\ddot{\boldsymbol{u}}_j\,\mathrm{d}m = \boldsymbol{0}$$

$$\boldsymbol{c}^{\times}\dot{\boldsymbol{V}}_0 + \boldsymbol{J}\dot{\boldsymbol{\omega}}_0 + \sum_j \int_j (\boldsymbol{b}_j^{\times}\boldsymbol{C}_{0j} + \boldsymbol{C}_{0j}\boldsymbol{r}_j^{\times})\ddot{\boldsymbol{u}}_j\,\mathrm{d}m = \boldsymbol{0}$$

$$\boldsymbol{L}_j\boldsymbol{u}_j + \sigma_j\{\boldsymbol{C}_{j0}\dot{\boldsymbol{V}}_0 - (\boldsymbol{C}_{j0}\boldsymbol{b}_j + \boldsymbol{r}_j)^{\times}\boldsymbol{C}_{j0}\dot{\boldsymbol{\omega}}_0 + \ddot{\boldsymbol{u}}_j)\} = \boldsymbol{0} \tag{26}$$

Equations (26), in fact, govern the motion of a free spacecraft with cantilevered appendages, so the sought hinges-locked vehicle modes are the same as the unconstrained modes, as in Hughes.[3] The development here parallels that in the previous subsection on hinges-free modes. Accordingly, we introduce the following modal expansion:

$$\boldsymbol{V}_0 = \dot{\boldsymbol{R}}_0 + \sum \boldsymbol{\chi}_{0\alpha}^c\dot{\eta}_\alpha^c(t), \qquad \sum = \sum_{\alpha=1}^{\infty} \tag{27a}$$

$$\boldsymbol{\omega}_0 = \dot{\boldsymbol{\Theta}}_0 + \sum \boldsymbol{\Phi}_{0\alpha}^c\dot{\eta}_\alpha^c(t) \tag{27b}$$

$$\boldsymbol{u}_j = \sum \boldsymbol{U}_{j\alpha}^c(\boldsymbol{r}_j)\eta_\alpha^c(t) \tag{27c}$$

where the superscript $c$ reminds us that these modal quantities pertain to constrained hinges. The quantities $\boldsymbol{\chi}_{0\alpha}^c$ and $\boldsymbol{\Phi}_{0\alpha}^c$ are the translation and rotation of the core body $B_0$ in $\alpha$th mode. Likewise, the eigenfunction $\boldsymbol{U}_{j\alpha}^c(\boldsymbol{r}_j)$ is the deformation of $E_j$ in the $\alpha$th mode, analogous to $\boldsymbol{U}_{jv}(\boldsymbol{r}_j)$ in the case of $v$th hinges-free mode, except that now a force is exerted at the hinge $0_j$ to ascertain that $\boldsymbol{U}_{j\alpha}^c(0_j) = \boldsymbol{0}$ and $\nabla_{\boldsymbol{U}}^{\times}{}_{j\alpha}^c(0_j) = \boldsymbol{0}$. The total motion of $j$th appendage relative to the $B_0$-fixed frame in $\alpha$th vehicle mode is denoted $\boldsymbol{W}_{j\alpha}^c(\boldsymbol{r}_j)$ and it may be expressed as

[cf. Eq. (16)]

$$W^c_{j\alpha}(r_j) \triangleq \chi^c_{0\alpha} - (b_j + C_{0j}r_j)^{\times}\Phi^c_{0\alpha} + C_{0j}U^c_{j\alpha}(r_j) \tag{28}$$

The $\alpha$th mode of the core body $W^c_{0\alpha}(r_0)$, on the other hand, is represented by

$$W^c_{0\alpha}(r_0) \triangleq \chi^c_{0\alpha} - r_0^{\times}\Phi^c_{0\alpha} \tag{29}$$

Thus, like Eq. (18), the $\alpha$th mode $W^c_{\alpha}(r)$ will be $W^c_{0\alpha}(r_0)$ or $W^c_{j\alpha}(r_j)$ depending on the domain under consideration. Orthogonality of these modes with the six rigid modes **1** and $-r^{\times}$, similar to Eqs. (19a) and (19b), can be proved readily. To express these conditions in terms of hinges-locked modal momenta coefficients, we define [cf. Eq. (20)]:

$$p^c_{j\alpha} \triangleq \int_j U^c_{j\alpha}(r_j)\,dm \qquad h^c_{j\alpha} \triangleq \int_j r_j^{\times} U^c_{j\alpha}(r_j)\,dm$$

$$p^c_{\alpha} \triangleq \sum_j C_{0j}p^c_{j\alpha} \qquad h^{0c}_{\alpha} \triangleq \sum_j (b_j^{\times} C_{0j}p^c_{j\alpha} + C_{0j}h^c_{j\alpha}) \tag{30}$$

Then, the abovementioned orthogonality is [cf. Eq. (21)]:

$$m\chi^c_{0\alpha} - c^{\times}\Phi^c_{0\alpha} + p^c_{\alpha} = 0, \qquad c^{\times}\chi^c_{0\alpha} + J\Phi^c_{0\alpha} + h^{0c}_{\alpha} = 0 \tag{31}$$

A counterpart of Eq. (19c) or (21c) does not exist in the case of hinges-locked modes inasmuch as, by definition of such modes, the body $E_j$ is constrained from turning at the hinge $0_j$. The eigenvalue problem obeyed by an $\alpha$th mode $W^c_{j\alpha}(r_j)$ and its orthogonality with a $\beta$th mode are furnished in Ref. 9.

With the aid of the expansion [Eq. (27)], momental properties [Eq. (31)], and orthogonality properties, the continuum equations [Eqs. (6) and (7)] are discretized to

$$m\ddot{R}_0 - c^{\times}\ddot{\Theta}_0 - \sum_j C_{0j}c_j^{\times}\dot{\Omega}_j = f(t) \tag{32a}$$

$$c^{\times}\ddot{R}_0 + J\ddot{\Theta}_0 + \sum_j C_{0j}J_{0j}\dot{\Omega}_j = g(t) \tag{32b}$$

$$c_j^{\times}C_{j0}\ddot{R}_0 + J_{0j}^T C_{j0}\ddot{\Theta}_0 + J_j\dot{\Omega}_j + \sum_{\alpha} h^{cI}_{j\alpha}\ddot{\eta}^c_{\alpha} = g_{0j} + g_j$$

$$(j = 1,...,N) \tag{32c}$$

$$\sum_j (h^{cI}_{j\alpha})^T\dot{\Omega}_j + \ddot{\eta}^c_{\alpha} + \omega^{c2}_{\alpha}\eta^c_{\alpha} = \chi^{cT}_{\alpha 0}f + \Phi^{cT}_{\alpha 0}g + \gamma^c_{\alpha}(t) \tag{32d}$$

where $\omega^c_{\alpha}$ is the frequency of the $\alpha$th hinges-locked mode. Unlike the hinges-free set of discrete equations [Eqs. (22)], the articulation motion Eq. (32c) and the modal coordinate $\eta^c_{\alpha}$ Eq. (32d) involve a coupling term called "inertial modal angular momentum coefficient" $h^{cI}_{j\alpha}$ defined as

$$h^{cI}_{j\alpha} \triangleq \int_j r_j^{\times} C_{j0}W^c_{j\alpha}(r_j)\,dm$$

$$= c_j^{\times}C_{j0}\chi^c_{0\alpha} + (J_jC_{j0} - c_j^{\times}C_{j0}b_j^{\times})\Phi^c_{\alpha 0} + \int_j r_j^{\times}U^c_{j\alpha}\,dm \tag{33}$$

which is different from $h^c_{j\alpha}$ and $h^{0c}_{\alpha}$ defined in Eq. (30). The disturbance input $\gamma^c_{\alpha}(t)$ to each $\alpha$th mode equals [cf. Eq. (23)]

$$\gamma^c_{\alpha}(t) \triangleq \sum_j \int_j U^{cT}_{j\alpha}(r_j)f_j(r_j,t)\,dA \tag{34}$$

To compact Eqs. (32) introduce

$$h^{cIT}_j \triangleq [...h^{cI}_{jv}...], \qquad h^{cI}_A \triangleq [h^{cI}_1...h^{cI}_N] \tag{35}$$

Recalling pertinent definitions from Eqs. (12), (13), and (24), Eqs. (32) then may be written in the more concise forms

$$M_{VV}\ddot{q}_{VR} + M^T_{VA}\dot{\Omega}_A = u_V(t) \tag{36a}$$

$$M_{VA}\ddot{q}_{VR} + J_A\dot{\Omega}_A + h^{cIT}_A\ddot{\eta}^c_e(t) = g_A(t) + g_{0A}(t) \tag{36b}$$

$$h^{cI}_A\dot{\Omega}_A + \ddot{\eta}^c_e(t) + \omega^2_c\eta^c_e(t) = \chi^c_0 f + \Phi^c_0 g + \gamma_c \tag{36c}$$

The vectors $\eta^c_e(t)$ and $\gamma_c(t)$ and the matrices $\omega_c$, $\chi^c_0$, and $\Phi^c_0$ are defined like their hinges-free companions in Eqs. (24).

## IV. Derivation of Identities

Our concern now is to compare hinges-free and hinges-locked modes for their accuracy in representing articulation motion. To address this concern, two approaches will be taken. First, an equation will be obtained from each of the above three sets of discrete equations that will be solely in terms of the articulation motion $\dot{\Omega}_A$ and stimuli. These three equations will then be compared to yield identities. In the second approach, three more equations will be derived from the three sets, each governing all $(6 + n_a)$ discrete degrees of freedom with flexible modal coordinates eliminated. Additional modal identities will be extracted by comparing these three equations. Laplace transformation plays a key role in this development.

### Identities Based on Articulation Motion Only

First, consider the discrete set [Eqs. (14)] based on appendage modes. By matrix manipulations, the following equation governing $\dot{\Omega}_A$ can be constructed readily:

$$[1 - \mathcal{H}^T_A(\mathcal{U}_{\infty} + \Omega^2_c/s^2)^{-1}\mathcal{H}_A\mathcal{J}^{-1}]\mathcal{J}\dot{\Omega}_A$$

$$= \mathcal{H}^T_A(\mathcal{U}_{\infty} + \Omega^2_c/s^2)^{-1}\mathcal{P}^0_A M^{-1}_{VV}u_V$$

$$- \mathcal{H}^T_A(\mathcal{U}_{\infty} + \Omega^2_c/s^2)^{-1}\gamma^a_A - M_{VA}M^{-1}_{VV}u_V + g_H \tag{37}$$

where $s$ is the Laplace variable; $\mathcal{H}_A$, theoretically, is an $\infty \times n_a$ matrix, and $\mathcal{U}_{\infty}$ an $\infty \times \infty$ symmetric matrix; $\mathcal{J}$ is an $n_a \times n_a$ inertia matrix, and $g_H$ is the total hinge torque vector:

$$\mathcal{H}_A \triangleq -\mathcal{P}^0_A M^{-1}_{VV}M^T_{VA} + H_A, \qquad \mathcal{U}_{\infty} \triangleq 1_{\infty} - \mathcal{P}^0_A M^{-1}_{VV}\mathcal{P}^{0T}_A$$

$$\mathcal{J} \triangleq J_A - M_{VA}M^{-1}_{VV}M^T_{VA}, \qquad g_H \triangleq g_A + g_{0A} \tag{38}$$

In Eqs. (38), $1_{\infty}$ is an $\infty \times \infty$ identity matrix. Thus, for an equation of $\mathcal{J}\dot{\Omega}_A(s)$, the coefficient of the hinge torque $g_H(s)$ will be

$$[1 - \mathcal{H}^T_A(\mathcal{U}_{\infty} + \Omega^2_c/s^2)^{-1}\mathcal{H}_A\mathcal{J}^{-1}]^{-1} \tag{39}$$

Anticipating our later needs, now we shall prove that

$$\lim_{s\to\infty}[1 - \mathcal{H}^T_A(\mathcal{U}_{\infty} + \Omega^2_c/s^2)^{-1}\mathcal{H}_A\mathcal{J}^{-1}]$$

$$= 1 - \mathcal{H}^T_A\mathcal{U}^{-1}_{\infty}\mathcal{H}_A\mathcal{J}^{-1} = 0 \tag{40}$$

Applying the matrix inversion lemma to $\mathcal{U}_{\infty}$, its inverse is found to be

$$\mathcal{U}^{-1}_{\infty} = 1_{\infty} - \mathcal{P}^0_A[\mathcal{P}^{0T}_A\mathcal{P}^0_A - M_{VV}]^{-1}\mathcal{P}^{0T}_A \tag{41}$$

On the other hand, owing to the identities $(D,E,F)''$ of Hughes[3]

$$\mathcal{P}^{0T}_A\mathcal{P}^0_A = \begin{bmatrix} m_e 1 & -c_e^{\times} \\ c_e^{\times} & J^0_e \end{bmatrix} \triangleq M^0_e \tag{42}$$

Also, by definition of $M_{VV}$ in Eq. (13) and virtue of Eqs. (1)

and (3)

$$M_{VV} = \begin{bmatrix} m_0 \mathbf{1} & -c_0^{\times} \\ c_0^{\times} & J_0 \end{bmatrix} + M_e^0 \triangleq M_0 + M_e^0 \tag{43}$$

which defines the mass matrix $M_0$ of the core body and reduces $\mathscr{U}_\infty^{-1}$ to

$$\mathscr{U}_\infty^{-1} = \mathbf{1}_\infty + \mathscr{P}_A^0 M_0^{-1} \mathscr{P}_A^{0T} \tag{44}$$

Next, we call upon the basic identities $(D,E,F)''$ of Hughes[3] again to derive the following new identities associated with the articulation degrees of freedom:

$$H_A^T H_A = J_A \qquad H_A^T P_A^0 = C_A^0 \qquad H_A^T H_A^0 = J_{0A}$$
$$\mathscr{H}_A^T \mathscr{H}_A = \mathscr{I} - M_{VA} M_{VV}^{-1} M_0 M_{VV}^{-1} M_{VA}^T$$
$$\mathscr{H}_A^T \mathscr{P}_A^0 = M_{VA} M_{VV}^{-1} M_0 \tag{I}$$

(New identities derived in this paper will be labeled with Roman numerals as they are cited.) These identities and Eq. (44), in turn, lead to the identity

$$\mathscr{H}_A^T \mathscr{U}_\infty^{-1} \mathscr{H}_A = \mathscr{I} \tag{II}$$

which proves Eq. (40).

Using the modal expansion [Eq. (15)], we obtain an equation analogous to Eq. (37) from the hinges-free discrete set [Eq. (25)]:

$$\mathscr{I}\dot{\Omega}_A = \mathscr{I}\Phi_A^T(\mathbf{1}_\infty + \omega^2/s^2)^{-1}(\chi_0 f + \Phi_0 g + \gamma) - M_{VA} M_{VV}^{-1} u_V(s) + [\mathbf{1} + \mathscr{I}\Phi_A^T(\mathbf{1}_\infty + \omega^2/s^2)^{-1}\Phi_A] g_H(s) \tag{45}$$

The coefficient of the hinge torque $g_H(s)$ in Eq. (45) equals Eq. (39). They both reduce to $\mathbf{1}$ as $s \to 0$. As $s \to \infty$, they yield, in view of Eq. (40), the identity

$$(\mathbf{1} + \mathscr{I}\Phi_A^T \Phi_A)^{-1} = \mathbf{0} \tag{III}$$

which proves a fortiori that because the inertia matrix $\mathscr{I}$ is positive definite and $\Phi_A^T \Phi_A$ nonnegative definite, the modal coefficients $\Phi_{jv}$ $(j = 1,...,N;\ v = 1,...,\infty)$ [Eq. (15)] constitute a nondiminishing series.

The hinges-locked discrete set [Eq. (36)] furnishes this equation for $\dot{\Omega}_A$:

$$[\mathbf{1} - h_A^{cIT}(\mathbf{1} + \omega_c^2/s^2)^{-1} h_A^{cI} \mathscr{I}^{-1}] \mathscr{I}\dot{\Omega}_A = g_H - M_{VA} M_{VV}^{-1} u_V - h_A^{cIT}(\mathbf{1} + \omega_c^2/s^2)^{-1}(\chi_0^c f + \Phi_{0g}^c + \gamma_c) \tag{46}$$

The equality of the coefficient matrices of $g_H(s)$ in Eqs. (45) and (46) gives rise to this identity in the $s$-domain:

$$[\mathbf{1} - h_A^{cIT}(\mathbf{1} + \omega_c^2/s^2)^{-1} h_A^{cI} \mathscr{I}^{-1}]^{-1} = \mathbf{1} + \mathscr{I}\Phi_A^T(\mathbf{1}_\infty + \omega^2/s^2)^{-1}\Phi_A \tag{IV}$$

As $s \to 0$, the left and the right side of Identity (IV) both degenerate to $\mathbf{1}$. On the other hand, taking the lim $s \to \infty$ of Identity (IV) and recognizing Identity (III), one may obtain the identity

$$[\mathbf{1} - h_A^{cIT} h_A^{cI} \mathscr{I}^{-1}] = \mathbf{0} \tag{V}$$

Identity (IV) can be rearranged such that it reveals poles and zeros of vehicle dynamics. For that, recognize that when $s = \pm j\omega_v$ $(v = 1,...,\infty;\ j^2 = -1)$ the right side of Identity (IV), which is also the coefficient of $g_H(s)$ in Eq. (45), is unbounded, so $\pm j\omega_v$ are the poles of the spacecraft. Consequently, for unboundedness to occur, the left side of Identity (IV), expressed in terms of individual hinges-locked modes, may be used to obtain the identity

$$\det\left[\mathbf{1} - \sum_\alpha (1 - \omega_\alpha^{c2}/\omega_v^2)^{-1} h_\alpha^{cI} h_\alpha^{cIT} \mathscr{I}^{-1}\right] = 0 \tag{VI}$$

where $h_\alpha^{cIT}$ is $\alpha$th row of the matrix $h_A^{cI}$. Similarly, when $s = \pm j\omega_\alpha^c$ $(\alpha = 1,...)$, the matrix within $[\cdot]$ on the left side of Identity (IV), which is the coefficient of $\mathscr{I}\dot{\Omega}_A$ in Eq. (46), is unbounded, which implies that $\pm j\omega_\alpha^c$ are the zeros of the dynamics. Therefore, to realize unboundedness, the inverse of the right side of Identity (IV) leads to

$$\det\left[\mathbf{1} + \sum_\mu (1 - \omega_\mu^2/\omega_\alpha^{c2})^{-1} \mathscr{I}\Phi_\mu \Phi_\mu^T\right] = 0 \tag{VII}$$

where $\Phi_\mu^T$ is the $\mu$th row of the matrix $\Phi_A$ [Eq. (24)]. Knowing the poles and zeros, Identity (IV), keeping in mind its lim $s \to \infty$, has this alternate form [cf. (Y) of Hughes,[3] which is slightly incorrect; see its correct form in the Appendix]:

$$[\mathbf{1} - h_A^{cIT} h_A^{cI} \mathscr{I}^{-1}]^{-1} \frac{\prod_{\alpha=1}^{n_f} (s^2 + \omega_\alpha^{c2})}{\prod_{\mu=1}^{n_f} (s^2 + \omega_\mu^2)} = [\mathbf{1} + \mathscr{I}\Phi_A^T \Phi_A] \frac{\prod_{\alpha=1}^{n_f} (s^2 + \omega_\alpha^{c2})}{\prod_{\mu=1}^{n_f} (s^2 + \omega_\mu^2)} \tag{VIII}$$

where $n_f$ is the total number of retained modes. Because of Identity (III) and Identity (V), however, this form seems to be less meaningful than the form of Identity (IV). Identities (VI) and (VII) are analogous to the identities $(M)_0$ and $(Q)$ of Hughes.[3] Under conditions of symmetry, these reduce to those concerned with individual articulation degrees of freedom

$$\sum_{\alpha_\ell=1}^{\infty} (1 - \omega_{\alpha_\ell}^{c2}/\omega_{\mu_\ell}^2)^{-1} [h_\alpha^{cI} h_\alpha^{cIT} \mathscr{I}^{-1}]_{\ell,k} = \delta_{\ell k} \tag{IX}$$

$$\sum_{\mu_\ell=1}^{\infty} (\omega_{\mu_\ell}^2/\omega_{\alpha_\ell}^{c2} - 1)^{-1} [\mathscr{I}\Phi_\mu \Phi_\mu^T]_{\ell,k} = \delta_{\ell k} \quad (\ell,k = 1,...,n_a) \tag{X}$$

where $\alpha_\ell = 1,2,...$ are the hinges-locked modes and $\mu_\ell = 1,2,...$ are the hinges-free modes that contribute to the $\ell$th articulation degree of freedom; $[\cdot]_{\ell,k}$ is the $(\ell,k)$ element of the matrix $[\cdot]$; and $\delta_{\ell k}$ is the Kronecker delta.

#### Identities Involving All Discrete Degrees of Freedom

Consider the discrete set [Eq. (14)] first. Collect all discrete degrees of freedom by defining:

$$\dot{q}_r \triangleq \begin{bmatrix} \dot{q}_V \\ \dot{\Omega}_A \end{bmatrix}, \qquad M_{rr} \triangleq \begin{bmatrix} M_{VV} & M_{VA}^T \\ M_{VA} & J_A \end{bmatrix}$$
$$\mathscr{P}_e \triangleq [\mathscr{P}_A^0 \quad H_A], \qquad u_r \triangleq \begin{bmatrix} u_V \\ g_H \end{bmatrix} \tag{47}$$

Next, take Laplace transform of Eqs. (14), assuming that there are no distributed forces on the appendages, and eliminate the appendage modal coordinate vector $Q_A(s)$ from Eqs. (14a) and (14b) by using Eq. (14c); one then arrives at

$$s^2 q_r(s) = M_s^{-1}(s^2) u_r(s) \tag{48}$$

where

$$M_s(s^2) \triangleq M_{rr} - \mathscr{P}_e^T(\mathbf{1}_\infty + \Omega_c^2/s^2)^{-1} \mathscr{P}_e \tag{49}$$

To derive the modal identities related to $q_r$, determine $dM_s^{-1}(s^2)/ds^2$, following Hughes[3]; that results in

$$\left.\frac{dM_s^{-1}(s^2)}{ds^2}\right|_{@\, s=0} = M_{rr}^{-1}\mathcal{P}_e^T\Omega_c^{-2}\mathcal{P}_e M_{rr}^{-1} \tag{50}$$

Now consider the hinges-free set [Eq. (22)] and the corresponding modal expansion [Eq. (15)]. They lead to equations similar to Eqs. (48–50). To eliminate the modal coefficients $\chi_{0v}$, $\Phi_{0v}$, and $\Phi_{jv}$ from these equations in favor of modal momenta coefficients $p_v$, $h_v^0$, and $h_{jv}$, the zero momentum properties [Eq. (21)] are utilized to find:

$$[\chi_0\ \Phi_0\ \Phi_A] = -\not{p}_e M_{rr}^{-1} \tag{51}$$

where the modal momentum coefficient matrix $\not{p}_e$ is

$$\not{p}_e \triangleq [p\ h^0\ h_A], \qquad p^T \triangleq [...p_v...], \qquad h^{0T} \triangleq [...h_v^0...]$$
$$h_j^T \triangleq [\cdots h_{jv} \cdots], \qquad h_A \triangleq [h_1 \cdots h_N] \tag{52}$$

The hinges-free counterpart of Eq. (50) is then:

$$\left.\frac{dM_s^{-1}(s^2)}{ds^2}\right|_{@\, s=0} = M_{rr}^{-1}\not{p}_e^T\omega^{-2}\not{p}_e M_{rr}^{-1} \tag{53}$$

The calculations for the hinges-locked complement of Eqs. (50) and (53) are tedious, inasmuch as in Eqs. (32) or (36) the rigid mode variables $\dot{R}_0$ and $\dot{\Theta}_0$ and the elastic modal coordinates $\eta_\alpha^c$ ($\alpha = 1,...,\infty$) are coupled with the physical articulation rates $\Omega_j$ ($j = 1,...,N$). The steps, nonetheless, are as follows. First, $\ddot{\eta}_e^c$ is eliminated from Eq. (36b) by using Eq. (36c). Uncoupled expressions for $q_{VR}(s)$ and $\Omega_A(s)$ are then obtained in terms of inertia parameters and the stimuli $u_V(s)$ and $g_H(s)$. The modal expansion (27a) and (27b) is used next to obtain the vehicle motion vector $q_V$ as a function of inertia matrices and $u_V(s)$ and $g_H(s)$. While doing so, the modal coordinate vector $\eta_e^c(s)$ and the inherently coupled articulation vector $\Omega_A(s)$ are eliminated again by using the earlier equations. Arranging $s^2 q_V(s)$ and $s\Omega_A(s)$ in the form of Eq. (48), a matrix equivalent to $M_S^{-1}(s^2)$ is obtained. The lengthy operation of $d/ds^2$ ($@\, s = 0$) on that matrix yields another matrix that is pre- and postmultiplied with $M_{rr}$ to prove that

$$\left.\frac{dM_s^{-1}(s^2)}{ds^2}\right|_{@\, s=0} = M_{rr}^{-1}\not{p}_e^{cT}\omega_c^{-2}\not{p}_e^c M_{rr}^{-1} \tag{54}$$

where the hinges-locked momentum coefficient matrix $\not{p}_e^c$ is [cf. Eq. (52)]

$$\not{p}_e^c \triangleq [p^c\ h^{0c}\ h_A^c], \quad p^{cT} \triangleq [...p_\alpha^c...], \quad [h^{0c}]^T \triangleq [...h_\alpha^{0c}...]$$
$$h_j^{cT} \triangleq [...h_{j\alpha}^c...], \quad h_A^c \triangleq [h_1^c...h_N^c] \tag{55}$$

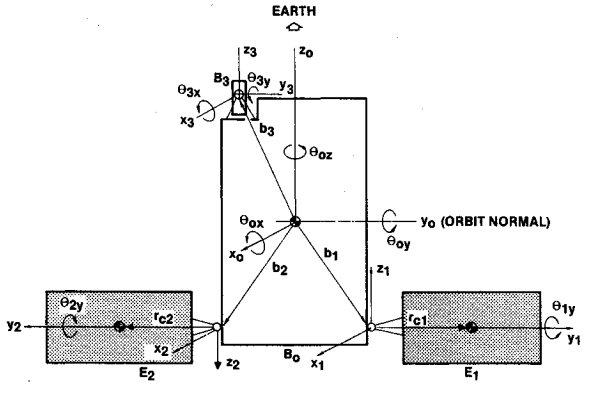


**Fig. 2 Four-body deformable spacecraft.**

In deriving Eq. (54), the matrix versions of the hinges-locked zero momentum properties of Eq. (31) are used to substitute $\chi_{0\alpha}^c$ and $\Phi_{0\alpha}^c$ in terms of $p_\alpha^c$ and $h_\alpha^{0c}$:

$$[\chi_0^c\ \Phi_0^c] = -[p^c\ h^{0c}]M_{VV}^{-1} \tag{56}$$

[cf. Eq. (51)]. Besides, the inertial modal angular momentum coefficient $h_{j\alpha}^{cI}$ is also replaced in terms of the coefficient $h_{j\alpha}^c$ by constructing the matrix version of the definitions in Eq. (33):

$$h_A^{cI} = [\chi_0^c\ \Phi_0^c]M_{VA}^T + h_A^c \tag{57}$$

A comparison of Eqs. (50), (53), and (54) allows us to write the desired identity

$$\mathcal{P}_e^T\Omega_c^{-2}\mathcal{P}_e = \not{p}_e^T\omega^{-2}\not{p}_e = \not{p}_e^{cT}\omega_c^{-2}\not{p}_e^c \tag{XI}$$

Identity (XI) is a generalization of Identities (V), (W), and (X) of Hughes,[3] for the former applies to spacecraft with articulated bodies, whereas the latter to spacecraft with cantilevered appendages.

Comments on the relative usefulness of Identities (I–XI) are now in order. Identities (I–III) and (V) involve modal coefficients and inertia parameters only, no frequencies, because these were obtained by taking the lim $s \to \infty$, and by doing so the spacecraft response at $t = 0^+$ is approached—at $t = 0^+$ the frequency or the strain energy of the structure has not had time to influence the response. Exact satisfaction of such identities usually requires a great many modes (Hughes[4]), and sometimes, for a real, complex elastic spacecraft, even an approximate satisfaction with the available modes from NASTRAN is infeasible. Nonetheless, because these identities do not involve frequencies, they are severe indexes to measure the fidelity of a math model. They are useful in deriving other important identities, though. Identities (VI–X), which involve both hinges-free and hinges-locked frequencies, are special forms of the matrix Identity (IV) in $s$ domain. Identities (VI) and (IX) represent, in hinges-locked modes, the motion at hinges resulting from an excitation at a hinges-free frequency. In contrast, Identities (VII) and (X) represent, in hinges-free modes, the hinge motion resulting from an excitation at a hinges-locked frequency. These identities are particularly suitable for numerically determining hinges-free modal parameters from hinges-locked parameters or vice versa. Considering the last identity, Identity (XI), its unique features are 1) each side of Identity (XI) includes modal coefficients as well as frequencies of only one kind, and 2) they apply to all $(6 + n_a)$ discrete degrees of freedom of the spacecraft. Furthermore, unlike Identities (VI–X), Identity (XI) is not the response at a particular excitation frequency; rather, according to Identities ($H$,$I$,$J$) of Hughes,[3] each side of Identity (XI) is related to the double integrals of the zero, first, and second moments of the flexibility kernels of the appendages, weighted by their mass distributions, and indeed it is a measure of steady-state step response of elastic modes in all discrete degrees of freedom. Thus, each identity serves a different purpose, although Identity (XI) is probably the best because of its just-mentioned unique features.

## V. Illustration of Identities and Discussion

The identities will now be illustrated for a four-body deformable spacecraft shown in Fig. 2. It has two flexible solar arrays, $E_1$ and $E_2$, each having one articulation degree of freedom about the $y_1$ and $y_2$ axis relative to the core body $B_0$, and a sensor having two rotational degrees of freedom about the $x_3$ and $y_3$ axis. These four articulation angles ($n_a = 4$) are denoted $\theta_{1y}$, $\theta_{2y}$, $\theta_{3x}$, and $\theta_{3y}$, and the spacecraft thus has 10 rigid modes. Hinges-free and hinges-locked vehicle modal data for the spacecraft were obtained using NASTRAN. Space limitations forbid delving into the illustration of the modal coefficients and the verification of Identities (III) and

(V), but these are covered in the companion paper.[9] Figure 3a of Ref. 9 confirms the prediction from Identity (III) that the hinges-free modal coefficients, in this case $\Phi_{1\mu y}$ ($\mu = 1,...,63$) for the $y_1$-solar array, form a nondecreasing series. The largest modal coefficients $\Phi_{1\mu y}$ for $\mu = 8,11,18,28,...$ correspond to those vehicle modes that predominately entail torsion of the $y_1$ array about the $y_1$ axis. In contrast, those contributing to $\theta_{3y}$, namely, $\Phi_{3\mu y}$ ($\mu = 1,...,63$), form essentially a decreasing series (see Ref. 9) because the sensor is rigid, and symmetric transverse bending of the arrays or local high-frequency deformation of $B_0$ at the sensor base produces $\Phi_{3\mu y}$ ($\mu = 1,\ldots,63$). The coupling coefficients $h^{cI}_{1\alpha y}$ for $y_1$ array rotation for the hinges-locked modes $\alpha = 1,\ldots,67$ are displayed in Fig. 4a of Ref. 9. Unlike $\Phi_{1\mu y}$, $h^{cI}_{1\alpha y}$ diminish with frequency. For $h^{cI}_{3\alpha y}$, see Fig. 4b of Ref. 9.

Identity (III) is illustrated in Fig. 5 of Ref. 9. Let the error indexes $e^{HF}_{kk}$ ($k = 1,3$) (HF = hinges-free) denote the corresponding diagonal elements of the $(4 \times 4)$ matrix $[1 + \mathcal{J}\Phi^T_A\Phi_A]^{-1}$. In contrast to their zero ideal value, the asymptotes of these indexes are 0.0406 for $k = 1$ ($\theta_{1y}$ rotation of the $y_1$ array) and 0.689 for $k = 3$ ($\theta_{3x}$, the $x$ rotation of the sensor). For $\theta_{1y}$, the error index $e^{HF}_{11}$ diminishes at the torsional modes $\mu = 8,11,18,28,....$ The error index for the $y_2$-array motion ($k = 2$) is the same as that for $k = 1$, except that it decreases instead at the adjacent torsional modes $\mu = 7,12,19,29,....$ Surprisingly, the asymptote of the error index for $\theta_{3y}$($k = 4$) hovers at 0.9976 instead of decreasing to its ideal value of zero. Figure 6 of Ref. 9 illustrates the hinges-locked identity [Identity (V)], rearranged as $\mathbf{h}^{cIT}_A\mathbf{h}^{cI}_A\mathcal{J}^{-1} = \mathbf{1}$. For discussing this identity and the ones following, define a "completeness index $\mathcal{C}$," which approaches unity for an error-free model. [The completeness index associated with the error index $e^{HF}_{kk}$ is $(1 - e^{HF}_{kk})$.] The growth of the diagonal elements (1,1) and (4,4) of the matrix $\mathbf{h}^{cIT}_A\mathbf{h}^{cI}_A\mathcal{J}^{-1}$ are depicted in Fig. 6 of Ref. 9. Surprisingly, alongside the slow decrease of the error index $e^{HF}_{11}$ in Fig. 5. of Ref. 9, $\mathcal{C}^{HL}_{11}$ (HL = hinges-locked) approaches unity in just two hinges-locked torsional modes, 5 and 6, and its asymptotic value is 1.029. Furthermore, by contrast with the hinges-free completeness index $\mathcal{C}^{HF}_{44} = 0.0024$ (that is, the previously mentioned error index $e^{HF}_{44}$ of 0.9976), the hinges-locked completeness index $\mathcal{C}^{HL}_{44} = 0.9421$ in Fig. 6b of Ref. 9 is remarkable; in fact, the first hinges-locked mode, a symmetric transverse bending mode of the arrays, contributes a mighty share, 0.9412, to $\mathcal{C}^{HL}_{44}$.

The identities that involve frequencies as well are illustrated in this paper. First, consider Identity (VII), which is summed over all hinges-free modes ($\mu = 1,...,63$) for a specific $\omega^c_\alpha$. When $\omega_\mu$ and $\omega^c_\alpha$ are the same to several decimal places, it is difficult to verify this identity in this form. On the other hand, Identity (VIII) indicates that when $\omega_\mu$ and $\omega^c_\alpha$ are truly the same, the corresponding poles and zeros cancel each other without affecting the articulation dynamics. This occurs because that particular mode does not contribute to the articulation motion, so such a mode may be deleted from the study. In numerical work, however, true equality between two real numbers is difficult to establish. Besides, as will be seen shortly, for the example in hand, sometimes, even though $\omega_\mu$ and $\omega^c_\alpha$ are the same up to three or four decimal places, the minuscule difference between the two is still important for the verification of an identity. Consequently, the following results are obtained without truncating either modal set. Returning to Identity VII, one finds that when $\alpha > 9$, hinges-locked frequencies $\omega^c_\alpha$ are so close to a corresponding hinges-free frequency $\omega_\mu$ that the determinant, instead of being zero, becomes an arbitrarily large number. Among $\alpha = 1,...,9$, Identity (VII) is best satisfied with $\alpha = 7$ and next best with $\alpha = 2$ (see Table 1). The circumstances that produce these results are revealed by Identity (X). For a given $\omega^c_\alpha$, when all available hinges-free modes are added to calculate the $(\ell,k)$ element of the left side of (X), it is denoted $\mathcal{C}^{HF}_{\ell,k,asy}$ where asy = asymptotic value. Figure 3 shows $\mathcal{C}^{HF}_{\ell\ell,asy}$ for $\ell = 1$, 3, and 4. The ideal value of this index is unity; however, when $\omega_{\mu_\ell} \approx \omega^c_{\alpha_\ell}$ for some $\mu$ and $\alpha$, this index assumes an arbitrarily large value, and for plotting purposes, such large numbers are replaced by 2 without affecting their signs. In the left side of Fig. 3a, in the useful range 0–1, the maximum value of $\mathcal{C}^{HF}_{11,asy}$ concerning the $y_1$-array rotation, $\theta_{1y}$, is 0.45 for the hinges-locked mode $\alpha = 2$—a symmetric transverse bending mode of the arrays. On the other hand, the first torsional hinges-locked mode having significant coupling with the rotation $\theta_{1y}$ is $\alpha = 5$, but $\mathcal{C}^{HF}_{11,asy}$ corresponding to $\alpha = 5$ is 0.16, less than 0.451 for $\alpha = 2$. Intuitively, the index $\mathcal{C}^{HF}_{11,asy}$ for $\alpha = 5$ should be greater than that for $\alpha = 2$; this does not happen because the hinges-free frequency $\omega_1$ (0.25724 Hz) is close to $\omega^c_2$ (0.25719 Hz). To determine the contribution of individual hinges-free modes, $\mu$, the growth of $\mathcal{C}^{HF}_{11}$ with $\mu$ to the asymptotic value 0.451 for $\alpha = 2$ is shown in the right side of Fig. 3a. $\mathcal{C}^{HF}_{11}$ is found to escalate discretely at $\mu = 1,8,11,18,28,29,35,41,42,...$, which, except for $\mu = 1$, involves torsion of the array 1. The contribution 0.42 (Fig. 3a) from the hinges-free mode $\mu = 1$—a symmetric transverse bending mode of the arrays, like $\alpha = 2$ hinges-locked mode—is, however, extraordinarily large: 93%. Nevertheless, the bending mode $\mu = 1$ is not pertinent to the articulation motion $\theta_{1y}$, so $\mathcal{C}^{HF}_{11} = 0.451$ for $\alpha = 2$ cannot be accepted, and, instead, $\mathcal{C}^{HF}_{11} = 0.16$ for $\alpha = 5$, a torsional mode, is accepted. Next, consider the sensor motion $\theta_{3x}$. The corresponding index $\mathcal{C}^{HF}_{33,asy}$ shown on the left side of Fig. 3b is 1.0059 for $\alpha = 7$ [compare with $\mathcal{C}^{HF}_{11,asy}$, and recall from Table 1 the value 0.00415 of Identity (VII) for $\alpha = 7$]. The growth of $\mathcal{C}^{HF}_{33}$ vs $\mu$ for $\alpha = 7$ is displayed on the right side of Fig. 3b, where it is observed to become unity at once when $\mu = 4$. To understand this, note that both $\mu = 4$ and $\alpha = 7$ modes involve antisymmetric in-plane bending of the arrays—a motion that induces

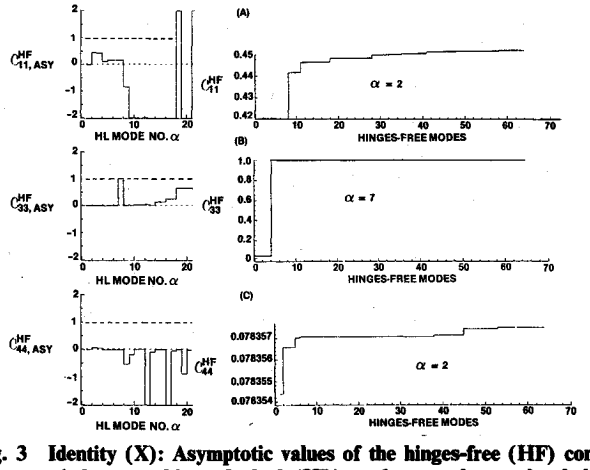


**Fig. 3 Identity (X): Asymptotic values of the hinges-free (HF) completeness indexes vs hinges-locked (HL) mode $\alpha$, and growth of this index vs hinges-free modes.**

**Table 1 Identity (VII): Variation of the hinges-free determinant with hinges-locked modes (ideal value = 0)**

| $\alpha$ | 1 | 2 | 3 | 4 | 5 | 6 | 7 | 8 | 9 |
|---|---|---|---|---|---|---|---|---|---|
| VII | 0.97105 | 0.04732 | 0.27012 | 0.79457 | 0.68305 | 0.68009 | −0.00415 | 0.19551 | −0.32426 |

Minimum value of the determinant, among the determinants for $\alpha = 10,...,63$, is 74.4, and the maximum value is $\infty$ when $\omega_\mu = \omega^c_\alpha$ up to several decimal places

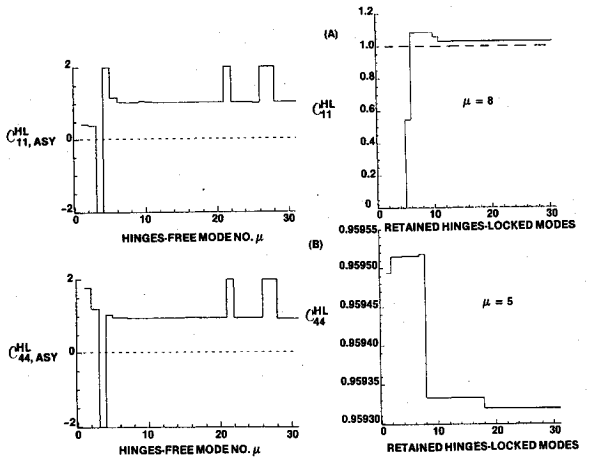


**Fig. 4 Identity (IX): Asymptotic values of the hinges-locked completeness indexes vs hinges-free modes, and growth of this index with hinges-locked modes.**

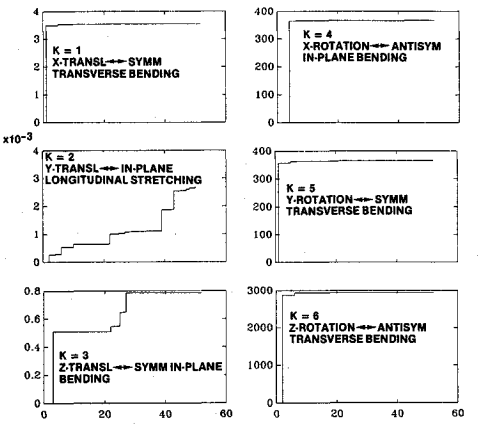


**Fig. 5a Hinges-free modes: Cumulative growth of the entries for spacecraft motion in the matrix $\not{p}_e^T \omega^{-2} \not{p}_e$.**

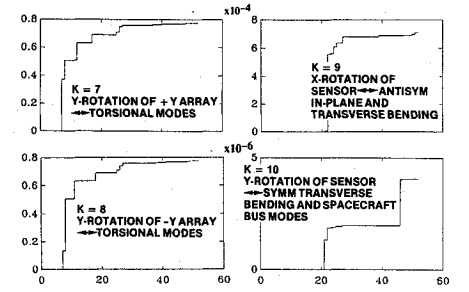


**Fig. 5b Hinges-free modes: Cumulative growth of the entries for articulation motion in the matrix $\not{p}_e^T \omega^{-2} \not{p}_e$.**

$\theta_{3x}$—and that $\omega_4 = 0.59541$ and $\omega_7^c = 0.59538$ Hz. When the rotation $\theta_{3x}$ of the rigid sensor is locked, the moment of inertia that must be turned by the antisymmetric in-plane bending is increased and that lowers the frequency commensurately. The ratio of the moment of inertia of the sensor and of the core body, both about $x_0$ axis, is 0.0717. The decrement of $3.0E-5$ Hz noted above in the frequency $\omega_4$ is mathematically so precise that $\mathscr{C}_{33}^{HF}$ becomes unity at once when $\alpha = 7$. Moreover, although $\omega_4$ and $\omega_7^c$ are the same up to three decimal places, the two modes cannot be truncated from the study of the verification of Identities (VII) and (X). Next, consider $\theta_{3y}$ rotation of the sensor—the rotation coupled with the transverse symmetric bending of the arrays. The associated index, $\mathscr{C}_{44,asy}^{HF}$, vs $\alpha$ is shown in Fig. 3c. In the range 0–1, the most it becomes is a startling low value: 0.07836 for $\alpha = 2$; for this $\alpha$, the growth of $\mathscr{C}_{44}^{HF}$ with $\mu$ indicates that 99.99% contribution arises from the first symmetric transverse bending mode $\mu = 1$.

The verification of Identity (IX), whose left side is now denoted $\mathscr{C}_{\ell k}^{HL}$, is considered in Fig. 4 for $\ell = k = 1$ and 4. Inasmuch as the hinges-locked coupling coefficients form a diminishing series, the determinant Identity (VI) and $\mathscr{C}_{\ell k,asy}^{HL}$ in Fig. 4 do not become arbitrarily large numbers once $\mu \geq 28$. Indeed, only for $\mu = 3,4,21,26,27$, is the index $\mathscr{C}_{\ell k,asy}^{HL}$ unbounded in contrast with the $\mathscr{C}_{11,asy}^{HF}$ in Fig. 3a, which is unbounded for all $\alpha \geq 9$. The index $\mathscr{C}_{\ell\ell}^{HL}$ depends on the selected hinges-free frequency $\omega_\mu$; for $\alpha$ having $\omega_\alpha^c > \omega_\mu$, the term $(1 - \omega_\alpha^{c2}/\omega_\mu^2)$ becomes negative and these particular hinges-locked modes diminish the sum. Focusing first on $\mathscr{C}_{11,asy}^{HL}$, surprisingly, it stabilizes early on to 1.05 when $\mu = 7$ or 8—the first hinges-free torsional mode. The ascent of $\mathscr{C}_{11}^{HL}$ to 1.05 for $\mu = 8$ with hinges-locked modes $\alpha$ (Fig. 4a) indicates significant contributions from $\alpha = 5$, 6, 10, and 11—all torsional modes; the contribution from higher torsional modes attenuates rapidly because of fast diminishing $h_{1\alpha y}^{cI}$. As for the rotation $\theta_{3y}$, the maximum value of $\mathscr{C}_{44,asy}^{HL}$, displayed in Fig. 4b, in the range 0–1 is 0.959 when $\mu = 5$—the second hinges-free symmetric transverse bending mode of the arrays. The growth pattern of $\mathscr{C}_{44}^{HL}$ vs $\alpha$ for $\mu = 5$, also shown in Fig. 4b, states that virtually the entire contribution arises from the first hinges-locked mode ($\alpha = 1$) involving symmetric transverse bending of the arrays.

From Identity (XI), only the $(6 + n_a, n_a = 4)$ diagonal entries of the $10 \times 10$ hinges-free matrix $\not{p}_e^T \omega^{-2} \not{p}_e$ are illustrated below. Earlier articulation motion labels $k = 1,2,3,4$ now become $k = 7,8,9,10$. Each diagonal term of the matrix $\not{p}_e^T \omega^{-2} \not{p}_e$ can be written as a summation over all available hinges-free modes, and Figs. 5 show the growth of each of those sums as the terms corresponding to each hinges-free mode ($\mu = 1,...,51$) are successively added. The asymptotic values of these nondecreasing sums depend on the degree of freedom under consideration, the interacting pattern of deformation (indicated in Fig. 5), and the double integrals of the corresponding zero and second moment of flexibility kernels weighted by the mass distribution. The vehicle's $x$ translation ($k = 1$), for example, interacts with symmetric transverse bending of the arrays. Now, $\mu = 1$ hinges-free mode having the lowest frequency (0.28 Hz) is a symmetric transverse bending mode. Because the arrays deform the most in this pattern, as compared to symmetric in-plane bending (interacting with $z$ translation, $k = 3$) or in-plane longitudinal stretching (interacting with $y$ translation, $k = 2$), the three corresponding asymptotic sums in Fig. 5a for $k = 1$, 3, and 2 also show the same descending sequence. Furthermore, for $x$ translation, most of the contribution stems from the first mode, whereas for $z$ translation four symmetric in-plane bending modes add up to almost the entire asymptotic sum. For $y$ translation, however, out of 51 modes, not one mode contributes significantly to this motion. The growth of the sums corresponding to the attitude motion ($k = 4,5,6$) are explained likewise. Regarding the articulation motion of the solar arrays ($k = 7,8$), out of 51, two groups of nearly seven torsional modes make up for most of the asymptotic sums (Fig. 5b). Compared to these sums, those corresponding to the motion of the sensor ($k = 9,10$) are three to five orders smaller (Fig. 5b) because the sensor is essentially rigid (so the flexibility kernel is essentially zero) and its moment of inertia is much smaller than those of other bodies.

Table 2 summarizes the completeness indexes for Identities (III), (V), (IX), and (X). Evidently, the hinges-locked indexes are far closer to unity than the hinges-free indexes, particularly so for the sensor motion. Moreover, the number of hinges-locked modes contributing significantly to the indexes is smaller than that for the hinges-free modes. These results indicate, at least for the spacecraft in hand, the superiority of

**Table 2 Summary of the completeness indexes for hinges-free and hinges-locked vehicle modes (ideal value = 1)**

| Hinges-free (HF) indexes | Identity (III), $1-e^{HF}_{\ell\ell,asy}$ | Identity (X) | Hinges-locked (HL) indexes | Identity (V) | Identity (IX) | Articulation motion | Associated mode of deformation |
|---|---|---|---|---|---|---|---|
| $\mathscr{C}^{HF}_{11,asy}$ | 0.9594 | 0.160 | $\mathscr{C}^{HL}_{11,asy}$ | 1.029 | 1.05 | $\theta_{1y}$ | Torsion |
| $\mathscr{C}^{HF}_{33,asy}$ | 0.311 | 1.0059 | $\mathscr{C}^{HL}_{33,asy}$ | TBD[a] | TBD[a] | $\theta_{3x}$ | Antisymmetric in-plane bending |
| $\mathscr{C}^{HF}_{44,asy}$ | 0.0024 | 0.0784 | $\mathscr{C}^{HL}_{44,asy}$ | 0.9421 | 0.9593 | $\theta_{3y}$ | Symmetric transverse bending |

[a]TBD = to be determined.

the hinges-locked modes to the hinges-free modes. We reiterate nevertheless that Identities (X) and (IX) [or (VII) and (VI)] represent two different situations as stated in the text, so a comparison of the indexes from these identities is slightly inappropriate perhaps. To form different groups of important hinges-locked modes for different discrete degrees of freedom, the right side of Identity (XI) can be used in a manner parallel to Fig. 5. When neither hinges-locked nor hinges-free modes are available, a few important appendage modes can be selected in accordance with Identities (I) or the left side of Identity (XI).

## VI. Conclusion

In a multibody spacecraft, the motion at a hinge is controlled by applying a torque, whereas, by definition, the hinges-free modes embody torque-free hinges; hinges-free modes, therefore, seem inherently deficient in representing a controlled motion at the hinges. Yet a controlled motion is not zero motion, so the hinges are somewhat free. The elastic part of that free motion is represented by the modal coefficients in the expansion of the articulation motion. These modal coefficients, unfortunately, do not diminish with frequency, so a large number of hinges-free modes must be retained in a high-fidelity simulation. In contrast, in the case of hinges-locked modes, the articulation motion has no modal expansion, and the torque at a hinge caused by the deformation of an articulated body is elegantly captured in the inertial modal angular momentum coefficients that diminish with frequency. Hinges-locked modes, therefore, are inherently well suited to represent a controlled motion at a hinge. The modal identities derived in this paper support this intuitive argument.

## Appendix: Correct Form of Identity (Y) of Ref. 3

Unless stated otherwise, the notations in this appendix are those of Hughes.[3] The denominator of the identity (Y) of Hughes,[3] the identity repeated here for convenience:

$$\bar{M}(s) \triangleq M_r \prod_{\alpha=1}^{\infty}(1+s^2/\omega_\alpha^2) \Big/ \sum_{n=1}^{N}\prod_{j=1}^{\infty}(1+s^2/\Omega_{jn}^2)$$

(for explanation of notations, see Hughes[3]) is slightly incorrect because, in this form, the denominator does not become zero at $k$th frequency of the $m$th appendage, $\Omega_{km}$—the product $\Pi_{j=1}^{\infty}(1+s^2/\Omega_{jm}^2)$ does become zero for $n=m$ but not for $n\neq m$. To determine the correct denominator, recognize that 1) it must become zero at each frequency of each appendage, and 2) the number of retained vehicle frequencies $N_r$ must be equal to the number of all retained appendage frequencies. Assuming that an equal number of frequencies of each appendage is retained, the correct form of the identity (Y) is then

$$\bar{M}(s) = M_r \prod_{\alpha=1}^{N_r}(1+s^2/\omega_\alpha^2) \Big/ \prod_{n=1}^{N}\prod_{j=1}^{N_r/N}(1+s^2/\Omega_{jn}^2) \qquad (Y')$$

Taking $\lim_{s\to\infty}\bar{M}(s)$ of (Y') above and recalling Eq. (83) of Hughes,[3] one obtains

$$M_0 = M_r \prod_{n=1}^{N}\prod_{j=1}^{N_r/N}\Omega_{jn}^2 \Big/ \prod_{\alpha=1}^{N_r}\omega_\alpha^2 \qquad (Z)$$

where the $6\times 6$ matrix $M_0$ is defined by Eq. (43) of this paper. Employing (Z), an alternate form of (Y') identity is obtained:

$$\bar{M}(s) = M_0 \prod_{\alpha=1}^{N_r}(s^2+\omega_\alpha^2) \Big/ \prod_{n=1}^{N}\prod_{j=1}^{N_r/N}(s^2+\Omega_{jn}^2) \qquad (Y'')$$

The identities (Y') and (Y'') are much simpler representations of poles and zeros of flexible spacecraft than that in Ref. 10.

## Acknowledgments

I wish to dedicate this paper to Professor Peter C. Hughes, Institute for Aerospace Studies, University of Toronto, Downsview, Ontario, Canada, for his invaluable help and for the enlightenment and inspiration his work has provided over the years. The numerical results in this paper were obtained by Thomas C. Witham, Avionics Systems Group, and Angela Lee, Guidance and Control Group. I thank both with pleasure for their conscientious efforts.

## References

[1]Likins, P. W., Ohkami, Y., and Wong, C., "Appendage Modal Coordinate Truncation Criteria in Hybrid Coordinate Dynamic Analysis," *Journal of Spacecraft and Rockets*, Vol. 13, No. 10, 1976, pp. 611–617.

[2]Hughes, P. C., and Skelton, R. E., "Modal Truncation for Flexible Spacecraft," *Journal of Guidance, Control, and Dynamics*, Vol. 4, No. 3, 1981, pp. 291–297.

[3]Hughes, P. C., "Modal Identities for Elastic Bodies with Application to Vehicle Dynamics and Control," *Journal of Applied Mechanics*, Vol. 47, March 1980, pp. 177–184.

[4]Hughes, P. C., "Space Structure Vibration Modes: How many exist? Which ones are important?" *Proceedings of the Workshop on Applications of Distributed System Theory to the Control of Large Space Structures,* Jet Propulsion Lab., California Inst. of Technology, Pasadena, CA, TR. 83-46, July 1983, pp. 31–47.

[5]Hablani, H. B., "Constrained and Unconstrained Modes: Some Modeling Aspects of Flexible Spacecraft," *Journal of Guidance, Control, and Dynamics*, Vol. 5, No. 2, 1982, pp. 164–173.

[6]Hablani, H. B., "Hinges-Free and Hinges-Locked Modes of Deformable Multibody Space Station—A Continuum Analysis," *Proceedings of the AIAA Dynamics Specialist Conference*, Monterey, California, AIAA 87-0925, April 1987, Pt. 2B, pp. 753–768; also *Journal of Guidance, Control, and Dynamics*, Vol. 13, No. 2, 1990, pp. 286–296.

[7]Hughes, P. C., *Spacecraft Attitude Dynamics*, Wiley, New York, 1986, pp. 70–76, Sec. 3.6.

[8]Hughes, P. C., "Dynamics of a Chain of Flexible Bodies," *Journal of the Astronautical Sciences*, Vol. 27, No. 4, 1979, pp. 359–380.

[9]Hablani, H. B., "Modal Identities for Multibody Elastic Spacecraft—An Aid to Selecting Modes for Simulation," AIAA Paper 89-0544, Jan. 1989.

[10]Okhami, Y., and Likins, P. W., "Determination of Poles and Zeros of Transfer Functions for Flexible Spacecraft Attitude Control," *International Journal of Control*, Vol. 24, No. 1, 1976, pp. 13–22.